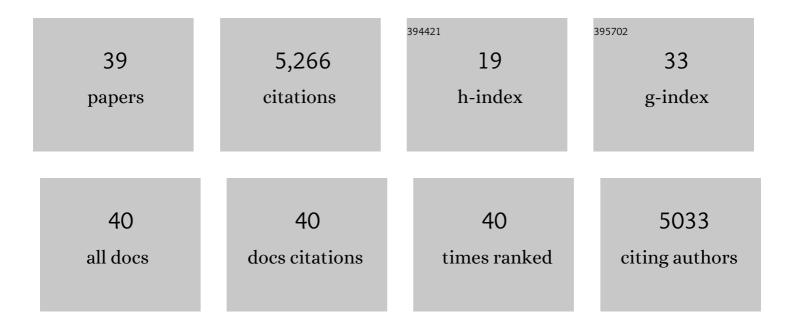
Hanqiu Xu

List of Publications by Year in descending order

Source: https://exaly.com/author-pdf/5821512/publications.pdf Version: 2024-02-01



ΗλΝΟΙΙΙ ΧΙΙ

#	Article	lF	CITATIONS
1	Modification of normalised difference water index (NDWI) to enhance open water features in remotely sensed imagery. International Journal of Remote Sensing, 2006, 27, 3025-3033.	2.9	3,361
2	A new remote sensing index for assessing the spatial heterogeneity in urban ecological quality: A case from Fuzhou City, China. Ecological Indicators, 2018, 89, 11-21.	6.3	294
3	Analysis of Impervious Surface and its Impact on Urban Heat Environment using the Normalized Difference Impervious Surface Index (NDISI). Photogrammetric Engineering and Remote Sensing, 2010, 76, 557-565.	0.6	270
4	Prediction of ecological effects of potential population and impervious surface increases using a remote sensing based ecological index (RSEI). Ecological Indicators, 2018, 93, 730-740.	6.3	234
5	Detecting Ecological Changes with a Remote Sensing Based Ecological Index (RSEI) Produced Time Series and Change Vector Analysis. Remote Sensing, 2019, 11, 2345.	4.0	220
6	Extraction of Urban Built-up Land Features from Landsat Imagery Using a Thematicoriented Index Combination Technique. Photogrammetric Engineering and Remote Sensing, 2007, 73, 1381-1391.	0.6	184
7	Urban Expansion and Heat Island Dynamics in the Quanzhou Region, China. IEEE Journal of Selected Topics in Applied Earth Observations and Remote Sensing, 2009, 2, 74-79.	4.9	83
8	The impact of impervious surface development on land surface temperature in a subtropical city: Xiamen, China. International Journal of Climatology, 2013, 33, 1873-1883.	3.5	76
9	A new remote sensing index based on the pressure-state-response framework to assess regional ecological change. Environmental Science and Pollution Research, 2019, 26, 5381-5393.	5.3	65
10	Derivation of Tasseled Cap Transformation Coefficients for Sentinel-2 MSI At-Sensor Reflectance Data. IEEE Journal of Selected Topics in Applied Earth Observations and Remote Sensing, 2019, 12, 4038-4048.	4.9	43
11	Rule-based impervious surface mapping using high spatial resolution imagery. International Journal of Remote Sensing, 2013, 34, 27-44.	2.9	41
12	Estimating ground-level PM2.5 over a coastal region of China using satellite AOD and a combined model. Journal of Cleaner Production, 2019, 227, 472-482.	9.3	39
13	Estimating PM2.5 concentrations in Yangtze River Delta region of China using random forest model and the Top-of-Atmosphere reflectance. Journal of Environmental Management, 2020, 272, 111061.	7.8	36
14	Development of a fine-scale discomfort index map and its application in measuring living environments using remotely-sensed thermal infrared imagery. Energy and Buildings, 2017, 150, 598-607.	6.7	35
15	Predicting effect of forthcoming population growth–induced impervious surface increase on regional thermal environment: Xiong'an New Area, North China. Building and Environment, 2018, 136, 98-106.	6.9	27
16	Built-up land mapping capabilities of the ASTER and Landsat ETM+ sensors in coastal areas of southeastern China. Advances in Space Research, 2013, 52, 1437-1449.	2.6	26
17	Characterizing bi-temporal patterns of land surface temperature using landscape metrics based on sub-pixel classifications from Landsat TM/ETM+. International Journal of Applied Earth Observation and Geoinformation, 2015, 42, 87-96.	2.8	26
18	Assessment of consistency in forest-dominated vegetation observations between ASTER and Landsat ETM+ images in subtropical coastal areas of southeastern China. Agricultural and Forest Meteorology, 2013, 168, 1-9.	4.8	20

Hanqiu Xu

#	Article	IF	CITATIONS
19	Incorporating residual temperature and specific humidity in predicting weather-dependent warm-season electricity consumption. Environmental Research Letters, 2017, 12, 024021.	5.2	19
20	Impervious Surface Information Extraction Based on Hyperspectral Remote Sensing Imagery. Remote Sensing, 2017, 9, 550.	4.0	19
21	A Remote Sensing Based Method to Detect Soil Erosion in Forests. Remote Sensing, 2019, 11, 513.	4.0	19
22	Remote sensing-based assessment of vegetation damage by a strong typhoon (Meranti) in Xiamen Island, China. Natural Hazards, 2018, 93, 1231-1249.	3.4	18
23	Lockdown effects on total suspended solids concentrations in the Lower Min River (China) during COVID-19 using time-series remote sensing images. International Journal of Applied Earth Observation and Geoinformation, 2021, 98, 102301.	2.8	18
24	The impact of building height on urban thermal environment in summer: A case study of Chinese megacities. PLoS ONE, 2021, 16, e0247786.	2.5	16
25	Markov chain analysis of vertical facies sequences using a computer software package (SAVFS): Courtmacsherry Formation (Tournaisian), Southern Ireland. Computers and Geosciences, 1998, 24, 131-139.	4.2	14
26	Spatial variability of urban climate in response to quantitative trait of land cover based on GWR model. Environmental Monitoring and Assessment, 2019, 191, 194.	2.7	13
27	Dynamic of soil exposure intensity and its effect on thermal environment change. International Journal of Climatology, 2014, 34, 902-910.	3.5	11
28	Estimating spatial variability of ground-level PM2.5 based on a satellite-derived aerosol optical depth product: Fuzhou, China. Atmospheric Pollution Research, 2018, 9, 1194-1203.	3.8	11
29	Anthropogenic Heat Flux Estimation Based on Luojia 1-01 New Nighttime Light Data: A Case Study of Jiangsu Province, China. Remote Sensing, 2020, 12, 3707.	4.0	10
30	Estimating PM2.5 concentrations in contiguous eastern coastal zone of China using MODIS AOD and a two-stage random forest model. Journal of Atmospheric and Oceanic Technology, 2021, , .	1.3	5
31	Fast Extraction of Built-up Land Information from Remote Sensing Imagery. Geo-information Science, 2010, 12, 574-579.	0.1	4
32	Comparison of Landsat-7 ETM+ and ASTER NDVI measurements. Proceedings of SPIE, 2010, , .	0.8	2
33	A study on the quantitative relationship between impervious surface and land surface temperature based on remote sensing technology. , 2016, , .		2
34	Automatic Absolute Radiometric Normalization of Satellite Imagery with ENVI/IDL Programming. , 2009,		1
35	The influence of urban reconstruction in urban heat island effect: Cangxia area of Fuzhou City, China. , 2010, , .		1
36	Remote sensing of urban expansion and heat island effect in Jinjiang estuary area of Fujian, China. , 2008, , .		0

Hanqiu Xu

#	Article	IF	CITATIONS
37	Urban major road extraction from IKONOS imagery based on modified texture progressing analysis technique. Proceedings of SPIE, 2009, , .	0.8	0
38	Remote sensing of impervious surface dynamics of Xiamen City, southeastern China. , 2011, , .		0
39	Urban road network extraction from IKONOS imagery based on multi-resolution analysis. , 2016, , .		0